https://doi.org/10.5194/egusphere-2022-533
Preprint. Discussion started: 12 July 2022

Spatial distribution of bedrock landslides over the landscape evolution in NW Himalayan River catchments

Abhishek Kashyap[1], Mukunda Dev Behera[1*], Anand K .Pandey[2], Ankit Agarwal[3]

[1]Centre for Oceans, Rivers, Atmosphere and Land Sciences (CORAL), Indian Institute of Technology Kharagpur, Kharagpur- 721302, West Bengal, India

[2]CSIR- National Geophysical Research Institute, Uppal Road, Hyderabad 500007, India

[3]Department of Hydrology, Indian Institute of Technology Roorkee, Roorkee-247667, Uttarakhand, India

*Corresponding Author: Mukunda Dev Behera: mdbehera@coral.iitkgp.ac.in

Emails:

Abhishek Kashyap: kashyap95abhishek@kgpian.iitkgp.ac.in

Anand K. Pandey**:** akpandey@ngri.res.in

Ankit Agarwal: ankit.agarwal@hy.iitr.ac.in

https://doi.org/10.5194/egusphere-2022-533
Preprint. Discussion started: 12 July 2022

ABSTRACT

The tectonically active North Western (NW) Himalaya landscape has evolved out of long-term active gradational interaction of major drainage systems. Landslides act as a primary erosion agent in these landscapes. We analyzed the spatial distribution of landslide occurrences along the Chenab, Beas, Sutlej, Yamuna, Ganga, and Kali rivers catchments in NW Himalaya to characterize landscape attributes. Further, spatial variability across different climatic zones viz., Western Disturbances –Indian Summer Monsoon (WD-ISM) was assessed. Seismicity and geochronological data were used to analyze the impact of bedrock landslides on landscape evolution. The denudation rate of the studied catchments was spatially correlated with exhumation age, precipitation intensity, and topographic variables. The highest probability of frequent landslides occurrence was found in the zones with ~24-32° of slope range, ~800-1200m of relief range, in 1200-2400m elevation range, which coincides with the precipitation erosivity range of ~1500-3000 mm/year in NW Himalayan river catchments. These zones also correlate well with the zones of cloudburst occurrences in NW Himalaya. Landslides in the Higher Himalaya, north of the MCT and across westerly dominated catchments such as Chenab, Beas, and Sutlej along the orographic barrier, are primarily triggered by higher tectonic activity. In contrast, landslides adjacent to the MCT in the front of the orographic barrier and across summer monsoon-dominated catchments such as Yamuna, Ganga, and Kali are controlled by litho-tectonics and mainly induced by higher precipitation intensity. It has been observed that catchments dominated by westerlies have a higher mean denudation rate and mean exhumation age than catchments driven by the Indian summer monsoon.

Keywords: Bedrock Landslides, Precipitation gradient, Topographic variables, NW Himalaya.

https://doi.org/10.5194/egusphere-2022-533
Preprint. Discussion started: 12 July 2022

1. INTRODUCTION

The steeped topography in a mountainous landform develops due to the interaction of tectonic forces that constitutes the surface uplift and the erosional process, associated with climate forcing (Champagnac et al., 2012). In any tectonically active landscape, landslides are act as the primary mass wasting process by which rock, soil and or debris moves downward due to action of gravity and the spatial interrelationship of tectonic and climate are considered as the principal driving agents in the controlling the distribution and frequency of landslides over landscape evolution (Gupta et al., 2018; 2019; 2022). Apart from tectonic and climate, the mass wasting process is controlled by the various local geomorphic and lithological agents such as slope distribution, relief, river morphology, structures and precipitation gradient and interaction of these agents with geological materials (Sanchez et al., 2010). The influence of tectonic on stream channel morphology is observable not only in the dimension, channel-width, and setting along the mountainous terrain, but over the normalized steepness of river profiles, the character of mountain slopes, and in the form of stream network that flow along regional lithological setup (Larsen & Montgomery, 2012). The mechanism of the bedrock landslides are considered as the primary process that respond to rapid incision over the development of the fluvial drainage network whereas the hillslope process are in general process (Korup et al., 2010). In general, topographic relief change, litho-tectonic setup, seismic distribution and climatic conditions, apart from the uncontrolled anthropogenic interference, are the common causes of initiation of bedrock landslides that have large socio-economic and environmental impacts.

The most significant component that affects sediment transport in moderate-to-steep topographic setups is erosion as a result of landslides or slope failure processes in the mountainous landscape (Ouimet et al., 2007; Broeckx et al., 2020). The long-term topographic growth process along non-glaciated fluvial landforms, is primarily governed by the connection between tectonic uplift and fluvial process dominated erosion (Whipple and Tucker, 1999; Wobus et al., 2006). In mountainous catchments, bedrock river channels incise into the bedrock terrain and operate as a transporting agent, conveying eroded sediment out of the mountain range and towards the ocean (Milliman and Meade, 1983; Campforts et al., 2020). These river incision processes prolong sediment transport, lowering the base level along adjacent hillslopes and causing slope failures (Campforts et al., 2020). This slope failure mechanism, on the other hand, obstructs downstream channels with eroded sediment and incorporates bedrock incision until landslide-derived sediment has been moved out of the system by mass wasting (Larsen

https://doi.org/10.5194/egusphere-2022-533
Preprint. Discussion started: 12 July 2022

and Montgomery, 2012; Ouimet et al., 2007; Korup et al., 2010; Shobe et al., 2016; Glade et al., 2019).

The interrelationship among landslides dynamics and fluvial mechanism in mountainous terrain is significant to understand the landscape evolution process and the corresponding sediment transport over the long-term scale (Pedersen & Egholm, 2013; Campforts et al., 2020). The growing understanding of the spatial distribution of landslides occurrence and there controlling variables has resulted in more efficient landslide susceptibility evaluation (Guzzetti et al., 2006), but procedure modulating landslide rate estimation (Broeckx et al., 2020) and landslide-driven sediment transport flux is not defined yet (Hovius et al., 2011; Croissant et al., 2017, 2019; Zhang et al., 2019; Broeckx et al., 2020). The impact of landslides on landscape evolution has been studied in many ways, including integrating river morphology with landslide dynamics and numerical simulations in a landscape evolution model (Densmore & Hovius, 2000; Champel et al., 2002; Egholm et al., 2013). The Numerical simulation of landscape attributes are significant tools to understand relationships between surface processes over long term spatio-temporal scales (Tucker and Hancock, 2010; Campforts et al., 2020). Both stream power and sediment transport via the downstream segment influence the fluvial incision. (Whipple et al., 2000; Hancock and Anderson, 2002; Turowski et al., 2007). The present study comprises the impact of bedrock landslides over the mechanism of landscape evolution process across the six major river catchments such as Chenab, Beas, Sutlej, Yamuna, Ganga and Kali in the NW Himalayan terrain.

1.1 Regional Geomorphic Setup

The landscape of a mountainous terrain is shaped by the drainage catchments and its basement tectonics (Jaiswara et al., 2019b). The Himalayan-Tibetan orogen system was formed by the intercontinental collision of the Indian and Eurasian litho-tectonic plates (Searle et al., 1997; Yin and Harrison 2000). The actively incising NW Himalayan mountainous landscape is geologically constituting the following litho-tectonic divisions, that are bounded by intracrustal thrusts and detachment faults namely; Indus Tsangpo Suture Zone (ITSZ) that represent the collision zones of these lithospheric plates (Yin and Harrison 2000), Tethyan Himalayan sequence that defines the northern boundary of ITSZ (Searle, 1986; Steck et al., 1998; Schlup et al., 2003), Higher Himalaya sequence that is bound by South Tibetan Detachment System (STDS) from north and Main Central Thrust (MCT) from south (Frank et al., 1973; Searle and Fryer, 1986; Walker et al., 1999; Miller et al., 2001; Vannay et al., 2004), the Lesser Himalaya sequence is limited on the south by Main Boundary Thrust (MBT) and on the north by the Main

https://doi.org/10.5194/egusphere-2022-533
Preprint. Discussion started: 12 July 2022

Frontal Thrust(MFT) along Outer/Sub Himalaya region (Miller et al., 2000; Vannay et al., 2004) (Fig.1c) . These litho-tectonic units have decreasing initiation ages from north to south (Orr et al., 2019, 2021). In tectonically active Mountainous region such as the western Himalaya, landslides are the most significant integrant of the orogeny (Korup et al., 2010). The western Himalayan landscape is evolved over several tectonically active faults and thrust system, and due to the much steeped topography along or close to these discontinuities setup, made these region highly unstable and vulnerable to hillslope failure (Gupta et al., 2017, 2019, 2022). This is also due to the litho-tectonic background of draining rock masses, as well as the disastrous geomorphic configuration of steep undulating slopes and higher relief ranges around these discontinuities (Gupta & Shah, 2008; Gupta et al., 2017).

Since in the NW Himalayan landscape, Landslides occurrence are often characterized by the two most prominent factor such as Seismically induced or either Precipitation induced slope failure process, but coupling of both the factor had a significant role on Topographic time scale (Roback et al., 2018). The majority of the western Himalayan region falls within seismic zones IV and V, indicating a high level of earthquake susceptibility. (Prakash S., 2013). The 1905 Kangra (M 7.8), 1934 Bihar (M 8.4), and 1950 Upper Assam (M 8.5) earthquakes are the most notable earthquakes of M > 8 that have occurred along the Himalayan arc in the last 100 years. (Seeber and Armbruster, 1981; Ambraseys and Bilham, 2000; Bilham et al., 2001). The previous studies in the Himalayan domain have defined geomorphic expressions such as displaced and warped late, evidence of paleo-lake formation due to movements along active faults, gullied surfaces marked by ravines and the development of canyons/deep narrow gorges, entrenched channels, and waterfalls, which are all indicative of active tectonics and fault displacement and its influence on the evolution of the landscape. (Seeber and Gornitz, 1983; Valdiya, 1996, 1999; Nakata, 1972; Malik and Nakata, 2003). As landslides are one of the most significant principal mass wasting process in tectonically active mountains (Ballantyne, 2002; Hovius, Stark, & Allen, 1997; Shroder & Bishop, 1998; Sanchez et al., 2010), the distribution and frequency of landslides are also considered to be driven by the climate. (Borgatti & Soldati; 2010). Although the proceeding precipitation before the earthquake events also makes the slopes more susceptible to landslide. The landslide distribution in the NW Himalayan region clusters to the south of the higher relief zone. The landslide clusters marks the zone of active erosions and has important role in landscape evolution. In the collisional orogeny, the spatial-temporal linkage of tectonics and climate has been observed frequently. Hillslope erosion is a

https://doi.org/10.5194/egusphere-2022-533
Preprint. Discussion started: 12 July 2022

significant factor in such interrelationships, notably when the surface imprints are landslides. (Ballantyne, 2002; Hovius et al., 1997; Korup et al., 2010).

The NW Himalaya terrain constitute large variations in relief (ranging >500-5000 m) from low lying valleys (close to mean sea level) to high elevated mountainous regions (ranging >7000m) as well as plateau regions (Fig. 1a), whereas higher relief zone >4 km and > 6 km elevation ranges coincides with the Higher Himalayan to lesser Himalayan zone. This zone of higher relief coincides with the zone of higher slopes, which varies from 0-85° (Fig. 1c). The high relief and high slope terrain in Higher to lesser Himalayan region are prone to slope instability.

1.2 Regional Climatic Setup

Since one of the most key parameters influencing erosion as a function of landslide drivers in any mountainous landscape is precipitation. The western Himalaya region witness two different sets of seasonal and spatial Variation in Orographic precipitation (Bookhagen et al., 2005a, 2005b; Bookhagen and Burbank., 2010; Dimri et al., 2018) classified as Western disturbance or Westerlies active during December-February month (Dimri et al., 2017) along the higher altitudes over the higher Himalayas and Indian Summer Monsoon dominant during June-September along the southern front (Bookhagen et al., 2005a). This precipitation correspondent act as a primary factor for the erosion and flooding in southern fronts of the Himalaya (Bookhagen al., 2004; 2005b) where landslides are the principal drivers. The Winter Precipitation occurs mainly in forms of snowfall between December and February in the Higher Himalayas and light to moderate precipitation over the outer Himalayas and the adjoining north Indo-gangetic plains and decreases with elevation (Singh and Kumar, 1997; Wulf et al., 2010; Dimri et al., 2015; 2017). However, the Indian summer monsoon accounts for intense precipitation during mid-July to mid-September and it is demonstrative focused in the elevation range of (1000±400m) and (2500±500m) in the southern Himalayan front (Fig. 1b) (Bookhagen & Burbank 2006; 2010). The Higher Himalaya with > 2000m topographic relief and >3000 m average elevation acts as topographic barrier that inhibits most summer monsoonal moisture to migrate northward into the orogeny and therefore creates a steep orographic precipitation gradient (Fig. 1a; 4a) (Bookhagen and Burbank, 2006; 2010). The annual precipitation during Indian summer monsoon decreases from >200mm towards southern mountain front to < 20 mm in the interior of the orogen within a spatial distance of <100-150 km (Bookhagen et al., 2005a; Wulf et al., 2010). Thus, while the spatial distribution

https://doi.org/10.5194/egusphere-2022-533
Preprint. Discussion started: 12 July 2022

of Indian Summer Monsoon & Western Disturbance Orographic Precipitation is critical to understanding Himalayan erosion on long and short timescales (Bookhagen et al., 2004; 2005b; 2011), the relationship between precipitation and Himalayan topography is still poorly defined. During the summer monsoon season, the intense seasonal precipitation leads in optimal river flows and sediment fluxes, and orographic processes result in noticeable spatial fluctuations in runoff magnitude, generating slope instability. (Bookhagen et al., 2004; Bookhagen & Burbank 2010).

The Indian summer monsoon is part of a larger event known as the Inter-Tropical Convergence Zone (ITCZ). The ITCZ distinguishes between wind motion projections in the southern and northern hemispheres. (Gadgil 2003; Bookhagen et al., 2005b). The latent heat released by moisture condensation exerted due to the relatively high Tibetan Plateau and the comparative warmth of the Asian mainland with the adjacent Indian oceans established the Indian Summer Monsoon circulation. (Webster et al., 1998; Bookhagen et al., 2005a). The summer monsoonal moisture are projected along the southern Himalayan front to the northwest, causing high intensified precipitation over the mountain front (Bookhagen & Burbank 2006). As the local topography controls the moisture transport along orographic barriers into deeply incised valleys perpendicular to the mountain front (Bookhagen et al., 2005b). This interrelationship between the moisture transport and topography controls the intensity and distribution of precipitation. The Summer Monsoon's high precipitation intensity exert a significant control over river discharge and sediment transport, resulting in major flooding and landslide activity along downstream over the southern part orographic barrier. (Bookhagen & Burbank 2006, 2010).

Although the southwest Indian summer monsoon and the westerlies have a differential impact on the western Himalayan region in the summer and winter months (Scherler et al., 2010; Wulf et al., 2010). The majority of precipitation that contributes to the annual mean occurs from June to September months along the southern front of the Himalayan foreland, when humid air masses from the Indian summer monsoon approach towards the Himalayan front (Bookhagen and Burbank, 2010). A substantial two-banded precipitation pattern coincides with the spatial heterogeneity along the south-east across-strike changes in surface elevation (Bookhagen and Burbank, 2006). The outer band of high rainfall (>250 mm/y) is found approximately north of the MBT in the Lesser Himalayas, whereas the inner band is found near the MCT at the geomorphic transition of the Lesser to the Higher Himalayas and is quite well expressed in the NW Himalayan bedrock river catchment (Bookhagen and Burbank, 2006, 2010). At elevations

https://doi.org/10.5194/egusphere-2022-533
Preprint. Discussion started: 12 July 2022

>3000 m, annual precipitation steeply decreases northward, whereas snowfall increases (Wulf et al., 2010), and vegetation cover gets gradually replaced by bare rock.

2. Hypothesis:

The bedrock landslides are the most significant component in the Himalayan terrain, controlling the surface process and exerting a strong influence on Himalayan hydrological budgets through terrestrial sediment transport, followed by bedrock river discharge. The landslide-derived sediment dynamics are aided by bedrock rivers in steep terrain. Understanding the landscape response towards the linkage of topographic-climatic attributes controlling the spatial distribution of landslides over the uplift-erosion setup in a tectonically active background involves analysing the interrelationship between these bedrock rivers and landslide process in the Himalayan terrain.

3. Materials & Methodology

We processed Open Source satellite derived SRTM - 30 meter; (http://srtm.csi.cgiar.org/) spatial Resolution topography Datasets for Landscape characterization and resampled the data using 'elevation void fill function' in ArcGIS to avoid null-error (Jarvis et al., 2008). We used the D8-algorithm to extract the drainage network (O'Callaghan and Mark, 1984) and drainage divide extraction of the major River systems (Chenab, Beas, Sutlej, Yamuna, Ganga, and Kali) taking MFT as a base level, in NW Himalaya. Precipitation data for the last 21 years (2001–2021) monthly datasets having 0.1° spatial Resolution from the Global Precipitation Measurement (GPM) have been obtained from (NASA – LP DAAC open source portal) to understand its role in regional gradation (erosion) process. Spatial landslides inventory datasets are obtained from Bhukosh portal of the Geological Survey of India **(**http://bhukosh.gsi.gov.in/) and spatial earthquake datasets are obtained from NASA-USGS open source platform (https://earthquake.usgs.gov). The geology, tectonic features and geographic location of denudation rates in the studied river catchments are compiled from previously published literatures (SM1).

In the present study we derived the topographic attributes such as slope, relief using elevation data and generate the seasonal and annual mean precipitation maps in GIS platform using ArcGIS. The relief map is generate by passing 900 m rectangular radius focal range window and the slope map by passing 500 m radius mean filter over the slope model from DEM owing to regional nature of present study (Jaiswara et al., 2019a, b). The geographic distribution of landslides points over the topographic attributes such as elevation, slope and relief as well as

Climatic attributes such as Precipitation gradient are extracted using "extract multi values to a point" tool in ArcGIS. Further the extracted gridded values datasets are evaluated through the statistical analysis in order to find highest probability density frequency for the spatial landslides occurrences over the topographic and climatic attributes in the studied bedrock river catchments in NW Himalaya. The quantitative landscape modeling through geomorphic indices from Digital Elevation Models are calculated in the MATLAB platforms using Transient-Profiler (Jaiswara et al., 2019a, 2020) and other tools (Schwanghart and Scherler, 2014). We evaluate the spatial interrelationship of regional landscape with the controlling attributes of bedrock landslides occurrences in NW Himalaya using following proxies.

3.1 Topographic distribution: Hypsometric Integral (Hi), slope frequency

In a drainage basin, the hypsometric integral (Hi) represents the relative distribution of elevation in a given area of the landscape. (Strahler, 1952). The Hi is a proxy for the basin's maturity stage since it describes the percentage area below the hypsometric curve that represents the volume of a basin that has not been eroded. (Strahler, 1952; Keller and Pinter, 2002). We derive slope frequency and hypsometry curves for the studied six river basins to characterize the spatial variation in the gradational response concerning the base level. These basic parameters define the broad evolutionary stage and the landscape's spatial variability and help assess variation in controlling factors (Strahler, 1952; Schumm, 1979).

$$\mathbf{Hi = (hmean - hmin) / (hmax+hmin)} \quad \ldots\ldots\ldots\ldots\ldots\ldots \text{(1)}$$

Where, Hi is the hypsometric integral and hmax, hmin, and hmean are the maximum, the minimum, and the mean elevation, respectively. Thus, high hypsometric integral indicates younger or youthful stage of landscapes while as intermediate to lower values for older ones as the landscape is denuded towards a stage of maturity and old stages (Strahler, 1952; Keller and Pinter, 2002).

3.2 Geophysical Relief- Minimum Eroded Rock Column

The geophysical relief of a region estimates a minimum cumulative eroded column in a landscape assuming a theoretical pre-incision surface, which is derived from the interpolation of the elevation from the current drainage divides to the corresponding riverbed with an assumption that the erosional process does not affect drainage divides (Abbott et al., 1997; Small and Anderson, 1998; Brocklehurst and Whipple, 2002). The spatial variability of the geophysical relief has been correlated with the Ksn and previously published denudation rates to understand long-term erosion localization across the studied river basin.

https://doi.org/10.5194/egusphere-2022-533
Preprint. Discussion started: 12 July 2022

In the present study we use a proxy to determine the exhumation age (Ma) of the studied catchments with observed sample locations using the denudation rate and geophysical relief. We divide the geophysical relief (m) of the observed sample location with the denudation rate (mm/y), to quantify the proxy exhumation rate using the relation (SM1):

$$\textbf{Exhumation rate} = ((GR*1000)/ DR)/ 10^6 \text{………} \quad (2)$$

Where; GR= Geophysical relief (m), DR= Denudation rate (mm/y)

3.3 Steepness index- slope-area analysis

The topographic relief of the erosional landscape is mostly determined by the shape of the river profile. The reference concavity (ref) was used to calculate a normalised steepness index (Ksn), which allows for a fair comparison across the basins despite their significantly different areas. (Wobus et al., 2006). Rivers tend to have a steady-state graded profile, which may be represented using the power law relationship between the local channel slope (S) along the river profile segment and the associated contributing drainage area (A) as follows: (Flint, 1974):

$$S = ksA^{-\theta} \text{…………} \quad (3)$$

Where *ks* (= [*U/K*] *1/n*) is the channel steepness index, θ [=*m/n*] is the channel concavity index, m and n are positive constants, *U* is the rock uplift rate (erosion rate (*E*) at a steady state), and *ks* represents the bedrock strength and/or climate.

4. Results

4.1 Landslides distribution over landscape characterization

The Western Himalayan region has higher frequency of landslides occurrence as compared to central and eastern Himalayan region, due to its higher relief change, slope gradient and topographic ruggedness. Since it was profound that the western Himalayas are climatically sensitive region, due to its setting near the consummation of the monsoon bearer belt, where changes in the strength of projection system of the summer monsoonal intensity and intensity of Western Disturbance interacts and their influence on orography growth processes can be examined (Bhatt and Nakamura., 2005). The spatial distribution of bedrock landslides in western Himalayan landscape shows the spatial contiguity of tectonics and Climatic linkage of the bedrock terrain in modulating surface process with landslides occurrence plotted over the

https://doi.org/10.5194/egusphere-2022-533
Preprint. Discussion started: 12 July 2022

studied River catchments area. We analyzed the landslides distribution as a function of erosion process in a River catchment scale to understand its role in the landscape evolution. The characteristic of spatial distribution suggest that the highest probability density frequency of landslides occurrence lies within ~24-32° of Slope range, ~800-1200 m of Relief range, in 1200-2400 m Elevation range, which coincides with the Precipitation erosivity range of ~1500-3000 mm/year (Fig. 2, 3).

The frequency distributions of landslides occurrences suggest the relative behaviour of erosion in a given bedrock river catchment (Stark and Hovius, 2001). In the western Himalayan catchments, the observed Weibull distribution and a power-law distribution of mean slope frequency and landslide occurrence frequency distribution imply a possible systematic mechanism for linking bedrock landslide dynamics in the landscape evolution process. (Iwahashi et al., 2003). To analyze the landscape association with the landslides occurrence in the NW Himalayan River catchments, we plotted the slope distribution pattern of the studied river catchments, which follows power-law with a bell-shaped slope frequency distribution (Burbank & Anderson 2013). The Yamuna, Ganga, and Kali in the high relief zone show a Gaussian distribution with a mean slope of ~25-30°, suggesting higher ruggedness. The slope frequency distribution of the Sutlej catchments show exponential distribution with over 50% area has average slope<10°, whereas Chenab and Beas showing Weibull distribution pattern with a mean slope of ~25-30° (Fig. A1b).

In order to understand the role of landslides distribution in the landscape evolution, we calculated hypsometric integral (Hi) (Strahler, 1952; Schumm, 1979) using hypsometric curves and plotted the Slope frequency distribution of the studied River catchments. The elevated landscape of western Himalayan River catchments such as Chenab and Sutlej show a youthful landscape with higher Hi values 0.43 and 0.57 respectively. Whereas the catchments Beas, Yamuna, Ganga and Kali showing a mature landscape with lower Hi such as 0.33, 0.30, 0.36, and 0.32, respectively° (Fig. A1a). The higher Hi values corresponds to a higher incision and landscape rejuvenation, which is also reflected in the relief and slope pattern. This suggest a spatial variation in erosional coupling with the active tectonics producing characteristic spatial variability in the landscape (Zeitler et al., 2014).

https://doi.org/10.5194/egusphere-2022-533
Preprint. Discussion started: 12 July 2022

4.2 Landslides process over the landscape evolution

In order to understand the tectonic association and the landscape response in the landslides process along the studied River catchments, the normalized steepness index (Ksn) had been used. The Ksn distribution over the mountainous terrain represent a constituent of the "stream power" and has been widely used as an erosion proxy to understand the active tectonics in River valleys (Flint, 1974; Howard & Kerby, 1983; Wobus et al., 2006; Gupta et al., 2018). Generally, it was suggested that the higher Ksn values indicates high uplift region and the lower Ksn indicates low uplift zones (Gupta et al., 2018). A normalized steepness index (Ksn) was computed at the reference concavity (θref) 0.45, which allows a fair comparison across all the catchments regardless their significantly varying areas (Wobus et al., 2006; Kirby and Whipple 2012) and has been used for determining the regional Ksn of the studied River catchments in NW Himalayan region. The spatial variability of the normalized Ksn for all the River catchments ranges from (4.5 – 1600) m, which has been correlated with the landsides and earthquakes occurrences over the topographic relief (Fig.4a). The spatial distribution of landsides occurrence correlated with higher Ksn values suggesting higher incision regime in a 200 km spatial buffer distance from MCT along the downstream. We characterize the Ksn values in Quantile distribution which classify the range of the observation into continuous intervals with equal probabilities. The Ksn distribution suggests that the downstream channel segments of the studied River catchments exhibit higher Ksn (> 252.8 m) suggesting higher dynamic incision (Fig. 4a); whereas the lower Ksn is observed in upper segments of the channel suggesting relative erosional quiescence. The Ksn values are overlaid over the topographic relief, which suggest that higher relief ranges proportionally correlates with high Ksn values along the STDS-MCT structural affinity. The spatial variability of topographic relief with the Ksn range suggest different characteristics in the studied catchments such as; First one in the Tethyan-Higher Himalayan sequence in the Sutlej catchments across STDS-MCT where Ksn achieves its highest values ranges ~ 252.8- 1600 m and relief ranges at ~ (2.5- 3.5) km. This zone is constrained with seismicity distribution in the litho-tectonic setup indicating active tectonics interference, which also act as the principal driver for the landslides initiation as a function of erosion along the downstream segment. Second one in the Upper Ganga-Kali catchment where relief range reaches maximum upto ~ (4-5) Km with corresponding Ksn ranges as (252.8- 1000) m. third one in the Chenab-Beas catchment where relief ranges (2-3) km with corresponding Ksn value ranges ~ (153.8 – 600) m. The amplitude of Ksn with corresponding relief decreases towards lower Himalayan sequence across MBT-MFT in the

https://doi.org/10.5194/egusphere-2022-533
Preprint. Discussion started: 12 July 2022

downstream segment. The spatial distribution of regional earthquakes in the higher Himalayas along the northern side of landslides occurrence over the litho-tectonic setup indicates as a major driving agent of in the topographic interference.

The Ksn distribution demonstrate the spatial erosion efficiency and the same can be estimated for a long period in the form of geophysical relief, which estimates the minimum eroded column considering the drainage divide in equilibrium (Abbott, 1997). The spatial variability of the geophysical relief has been correlated with the Ksn, Denudation rates and landslides datasets to understand long-term erosion localization across the studied River catchments. Three distinct area across the Studied River basin show a characteristics geophysical relief distribution ranges from (0-4) km, such as the Upper Ganga-Kali River segment across STDS and MCT structural affinity which shows maximum geophysical relief ranging ranges ~ (3-4) km, second along downstream segment of Sutlej River across MCT and MBT structural affinity which ranges ~ (2-3.5) km, and third along Beas and Chenab segment across MCT-MBT structural association which ranges < 3 km (Fig.4b). The geophysical relief in the Upper Ganga adjoining Kali catchments show maximum erosions which decreases southward to ~0-200 m along the MFT. The close association of high Ksn-geophysical relief with the active structures across the studied catchments with the cluster of landslides occurrence, we analyzed the spatial variation as the function of landslides driven incision to understand coupling of landslides dynamics and long erosion that may have implication on landscape evolution of the region (Clift et al, 2005; Saylor et al., 2010).

4.3 Landslides mechanism over orographic process

The rate of sediment production, the ability of sediment transport along channels, and the total contribution of landslides frequency to the sediment budget on a catchment scale are usually used to define the geomorphic control of bedrock landslides. (Korup et al., 2009). Within a given catchment, the amount of total sediment produced by bedrock landslides as a function of erosional proxy is a function of their frequency and amplitude. (Crozier and Glade, 1999; Reid and Page, 2003). Although, seismically or precipitation-induced landslide occurrence frequently produce higher incision rate through the sediment production in long-term catchment scale (Korup et al., 2009). However, in the short to long term scale, sediment transfer of landslide degraded material to the channel network may be considered a stochastic process. (Benda and Dunne, 1997; Tucker, 2004). In order to understand the role of landslides occurrence in mountain building process, we quantify the spatial interrelationship between previously published incision rate and exhumation age (Rao et al., 1997; Scherler et al., 2014;

https://doi.org/10.5194/egusphere-2022-533
Preprint. Discussion started: 12 July 2022

Morell et al., 2015; Bookhagen et al., 2016) dataset in the studied river catchments with geomorphic parameters and established the linkage between them (Fig.5). We characterize the obtained geochronology datasets in two category as first in westerlies dominated segment such as Chenab, Beas and Sutlej river catchments (Fig.5a, b, and c). Second in Indian summer Monsoon dominated segment such as Yamuna, Ganga and Kali river catchments (Fig.5d, e, and f). The statistical trend analysis of observed mean denudation rate and mean exhumation age between two segments suggest that the westerlies dominated catchments have relatively higher mean denudation rate as 0.5 mm/y and mean exhumation age as 4.5 Ma with respect to Indian summer monsoon dominated catchments which shows mean denudation rate as 0.3 mm/y and mean exhumation age as 3.5 Ma (Fig. 6a, b). For the westerlies dominated catchments the spatial interrelationship between denudation rate with exhumation age and annual mean precipitation suggest inverse proportional relationship between them as for the increase in denudation rate the exhumation age and annual mean precipitation decreases whereas with the topographic variables such as elevation, relief and geophysical relief suggest direct linear proportional relationship such that with the increase in denudation rate elevation, relief and geophysical relief increases. For the summer monsoon dominated catchments the spatial interrelationship between denudation rate with exhumation age suggest inverse proportional relationship between them as for the increase in denudation rate the exhumation age decreases whereas with the annual mean precipitation and topographic variables such as elevation, relief and geophysical relief suggest direct linear proportional relationship such that with the increase in denudation rate annual mean precipitation and elevation, relief and geophysical relief increases.

4.4 Landslides susceptibility in Western Himalayan catchments

Since in the recent times increased understanding of the spatial distribution of landslides occurrence over mountainous terrain has resulted in enhance assessments of landslide susceptibility analysis (Guzzetti et al., 2006), but mechanism modulating bedrock landslides as a function of an erosional proxy (Broeckx et al., 2020) and landslide-regulating sediment variability over catchment scale remain less understood yet (Hovius et al., 2011; Croissant et al., 2017, 2019; Zhang et al., 2019; Broeckx et al., 2020). The probability assessment of the spatial distribution of landslides occurrences using numerical models are significant tools to understand the linkage among the variables controlling surface processes and their interconnection over spatio-temporal scales (Tucker and Hancock, 2010). Here we derived the spatial landslides probability density using landslides occurrence grid values from topographic

https://doi.org/10.5194/egusphere-2022-533
Preprint. Discussion started: 12 July 2022

variables such as elevation, relief, slope and climatic variables such as annual mean precipitation. The obtained spatial probability density is the coupling spatial relationship of topographic variables and climatic variables. The obtained spatial landslides probability density is characterized into Quantile frequency distribution and integrated with Indian summer monsoon contour values which was obtained in mean occurrences of the trend analysis. The probability density of landslides occurrences suggest that the summer monsoon dominated catchments have higher probability distribution ranges (0.3-1) as compared to westerlies dominated catchments (Fig.7). Also ISM contour values 1000 mm/y and 2000 mm/y are correlating proportionally with highest frequency in the Ganga, kali and Yamuna river catchments whereas ISM contour intensity decreases and represent inverse proportional relationship along Chenab and Beas catchments whereas Sutlej catchment act as a orographic barrier differentiating the intensity of two seasonal distribution patterns on an annual scale. It was also concluded that the higher probability density is estimated into the spatial proximity of ~100-150 km between MCT and MBT lithological interference within lesser Himalayan sequence on the transect edge of higher Himalayas.

5. Discussion

5.1 Trend Analysis of landslides occurrences

The trend analysis of landslides occurrences over the western Himalayan river catchments suggest that the catchments which are influenced by Indian summer monsoon precipitation pattern such as Yamuna, Ganga and Kali catchments have higher frequency distribution of landslides occurrences as compared to westerlies dominated catchments due to their higher relief change, steeped slope gradient and maximum eroded rock column. For the topographic variables the mean trend of landslides occurrences lies in the range of 1000-2000 m for the elevation, ~800-1000 m for the relief and 20°-30° for the slope gradient. The upper extreme values are obtained in the Ganga and Sutlej catchments which have landslides occurrence at higher elevation ranges ~5000-6000m , relief ranges ~ 2000-2500 m and slope gradient ranges 50°-60°. For the precipitation context the mean trend of landslides occurrences lies in the range of 1500-2500 mm/y for the annual mean, ~500-1500 mm/y for the Indian summer monsoon period and 100-300 mm/y for the western disturbance period. The western disturbance trend over landslides occurrence clearly shows the decreasing trend of its intensity across west to east catchments whereas ISM suggest increasing trend of its intensity from west to east catchments. The observation suggested that the Higher Himalayan region serves as a critical orographic barrier, separating wet regions to the south from drier ones to the north. Although

https://doi.org/10.5194/egusphere-2022-533
Preprint. Discussion started: 12 July 2022

the Sutlej catchment serves as a climatic transition zone that alters the strength of the Indian summer monsoon by blocking monsoonal conveyor flux, precipitation intensity decreases and precipitation maxima shifts to lower elevations. However due to orographic lift phenomena the precipitation pattern shows two fold distribution in these sequences and significantly increased and produce substantial erosional in the form of debris flows as a function of bedrock landslides in the higher Himalayas on sparsely vegetated, steep hillslopes and higher relief zones. The observed mean precipitation was not significantly higher along the low to medium elevations. This shift has a profound impact on the Himalayan foreland's overall sediment budget.

Since active seismicity in the Higher-Tethyan Himalaya regions are observed over the clusters of earthquake events with the possible seismic triggering of large bedrock landslides along the downstream. In heavy monsoonal seasons, earthquakes play a limited role in tectonically modifying sediment quantities to bedrock rivers downstream. Although it has been suggested that there may be a delay between seismically-induced processes and sediment movement during heavy precipitation events, causing sediment transport to lower elevations to be substantially slowed. Since earthquakes are a significant factor for initiating bedrock landslides as a function of erosion in humid, medium-elevation regions, it may be assumed that earthquakes are a significant factor for initiating bedrock landslides as a function of erosion. (Bookhagen et al., 2005a). It was also proposed that the denudation rate is one of the most essential erosional hillslope processes in the Himalayan terrain's arid, high-elevation zones, which is strongly influenced by orographic lift during the monsoon season.

5.2 Spatial interrelationship of tectonic and climate linkage in initiating bedrock landslides

The Himalaya landscape is likely the one setting for improving our understanding of the spatial relationship between tectonics and climate-altering surface processes. Along the southern Himalayan mountain front, the interaction of topography and summer monsoonal flux controls precipitation gradient, stream outflow, and sediment movement (Bookhagen et al., 2004; 2005b). The relief formation of the landscape is primarily controlled by the fluvial bedrock incision which also profound control on limiting denudation rate process (Whipple and Tucker, 1999; Godard et al., 2004; Safran et al., 2005). The variation in fluvial incision rates is generally passively regulated by the hillslope growth process. Since there has been an increase in fluvial incision rates, nearby hillslopes have become steeper, which is countered by rapid bedrock landsliding. Apparently with the decrease in fluvial incision rates, or channel avulsion in

https://doi.org/10.5194/egusphere-2022-533
Preprint. Discussion started: 12 July 2022

downstream segment will reduce the relief structure which further minimize the rates of bedrock landsliding on the adjoining hillslopes. In the NW Himalayan River catchments the spatially uniform hillslope angles are formed by the close geomorphic channel-gradient coupling and the limiting hillslopes are at threshold slope angle for failure process (Burbank et al., 1996; Harvey, 2002). Slope distribution of the studied catchments are remarkably uniform except Sutlej catchment despite strong gradients in uplift rates, precipitation intensity, erosional efficiency, and lithological settings. The occurrence of such optimal hillslopes suggests that local topographic relief is a function of drainage density, but not fluvial incision rates or rock uplift (Burbank, 2002).Therefore, in the non-glaciated landscape the fluvial incision as the rate-limiting process would, control the sediment transport, considering complete geomorphic coupling between streams networks and slope gradient (Whipple and Tucker, 1999).

Tectonic induced climatic factors, according to several recent research, control the rates and patterns of denudation over the Himalayan landscape (Hodges et al., 2001, 2004; Burbank et al., 2003; Scherler et al., 2014; Godard et al., 2014; Morell et al., 2015). In our analysis, we observe that the climatically characterized catchment wise variability of denudation rates shows linear functional relationship with topographic variables and precipitation intensity for the summer monsoon dominated catchment and there should be inverse functional relationship with the exhumation age. The variability in the denudation rate trend decreases inversely as precipitation or exhumation age increases, for the westerlies dominated catchments (Fig.6). As a result, we infer that variation in denudation rates, as well as the linear or inverse functional relationship between topographic variables, precipitation intensity, and exhumation age, can be explained by tectonic effect or lithological interference. Furthermore, we believe that a number of factors are responsible for the variation in denudation rates and the relationship between denudation rates and topographic or climatic variables at the catchment scale, which serves as a key parameter in understanding the landslides dynamics process in landscape evolution.

We also calculate the spatial probability density using landslides occurrence grid values from the topographic variables and precipitation intensity within the studied catchment. The positive correlation of probability density is observe along summer monsoon dominated catchments such as Yamuna, Ganga and kali between landslides occurrence and ISM contour, which suggested that the spatial distribution of landslides occurrences are primarily control by summer monsoonal intensity along the southern Himalayan front (Fig.7) . Whereas studies in westerlies dominated catchments suggested that transitional orographic and climatically regimes from Sutlej catchment correspond to relative high mean denudation rates and exhumation age, profound less control of ISM intensity over bedrock landslides initiation. We analyzed the seasonal variation of Himalayan precipitation, that reflect that the seasonal intensity of precipitation along strike that caused by the higher impact of moisture flux from the Western disturbance in the western Himalaya (Barros et al., 2006), resulting in higher intensity of winter precipitation in westerlies dominated catchment with respect to the monsoon-dominated catchments in the east. Higher seasonality of precipitation and extreme precipitation events may drive higher and more variability in the denudation rates trend, even when total annual mean precipitation is relatively low (Snyder et al., 2003).

The observed relationship between denudation rates, slope gradient, and topographic variables is linear in the given tectonically active and climatically varying catchments, where denudation rates and exhumation age are inversely proportional to increased topographic steepness. Since the rising linear functional relationships in the Himalayan catchment show that bedrock landslides as a function of erosional proxy allows landscapes to become steep as a function of denudation rate. A change in the relative importance of topographic optimum values for slope failure might cause a shift in the linear relationship between topographic steepness and topographic or geophysical relief. (Burbank et al., 1996; Montgomery, 2001). As increase in denudation rates along the downstream segment, topography will adequate to continue the steepness process to a higher level and become susceptible to slope failure where optimum slope angles are reached earlier as denudation rates increase. We found that landslides occur more frequently when channel steepness increases in response to related slope gradient and denudation rates, implying a linear proportionate link between channel steepness index and denudation rates. The findings also imply that for places with the lowest precipitation rates, such as western disturbance dominated catchments, the mean denudation rates trend corresponds linearly with the mean exhumation age trend in order to provide surface runoff for catchment erosion efficiency. If precipitation intensity influences the erosional efficiency along a strike, the maximum denudation rates should be associated with high precipitation intensity, such as along the summer monsoon catchments. Although, it is considered that the mean annual precipitation may not be the primary driver to evaluate how precipitation intensity impacts denudation rates spatial variability. It has been suggested that the spatial variability of precipitation intensity over the seasonal distribution modulates erosion effectiveness in bedrock terrain (Lague et al., 2005).

6. Conclusion

The present study concluded that the spatial distribution of bedrock landslides occurrence over the controlling attributes such as topographic and precipitation variables show the highest probability of frequent landslides occurrence lies in the zones with ~24-32° of Slope range, ~800-1200 m of Relief range, in 1200-2400 m Elevation range, which coincides with the Precipitation erosivity range of ~1500-3000 mm/y in NW Himalayan River catchments. We analyzed the variability of denudation rate interrelationship with topographic variables, precipitation intensity and exhumation age over the studied river catchments along the western Himalayan landscape emphasise the significance of topographic-climate coupling in controlling the variability of denudation rates. We observe a strong linkage among the denudation rates pattern and the variables controlling distribution of bedrock landslides, such as topographic matrices and precipitation intensity which show direct proportional relationship across the summer monsoon dominated catchments whereas precipitation intensity relatively shows inverse proportional relationship across westerlies dominated catchment. In general our study remark the significance of spatial interrelationship of tectonic and Climatic linkage in understanding the relationship of bedrock landslides over landscape evolution in a tectonically active and highly dynamic orogen such as the western Himalaya. Furthermore, bedrock landslides and annual mean precipitation regulate the relationship among denudation rates and topographic variables in a highly active and dynamic orogen. The degree of linearity proportional relationship between denudation rate and topographic metrics such as slope gradient, topographic relief, geophysical relief, Ksn increases as mean annual precipitation increase. The observe outcome of our study is a more linear feedback of topography and topographic steepness to change in the denudation rates in lesser Himalayan sequence, whereas it shows nonlinear response in Higher to Tethyan Himalayan sequence. Further studies on how these bedrock landslides occurrence influence variation in denudation rates and topographic change in different tectonic setups will substantially increase our understanding of how these prominent earth surface processes associate worldwide.

Acknowledgments: The Authors acknowledge the authorities of IIT Kharagpur for facilitating the study. AK thanks the Ministry of Education, Government of India for the grant of a Ph.D. Research Fellowship. Geological Survey of India (GSI-Bhukosh portal) for providing landslides inventory datasets.

Conflict of interest: Authors declare that there is no potential conflict of interest.

https://doi.org/10.5194/egusphere-2022-533
Preprint. Discussion started: 12 July 2022

References

Abbott, L. D., Silver, E. A., Anderson, R. S., Smith, R., Ingle, J. C., Kling, S. A., Haig, D., Small, E., Galewsky, J., and Sliter, W. S.: Measurement of tectonic surface uplift rate in a young collisional mountain belt, Nature, 385, 501–507, https://doi.org/10.1038/385501a0, 1997.

Ambraseys, Nicholas, and Roger Bilham. "A Note on the Kangra Ms = 7.8 Earthquake of 4 April 1905." Current Science 79, no. 1 (2000): 45–50. http://www.jstor.org/stable/24103320.

Anon: Abbott, J. T. (1997). Late Quaternary alluviation and soil erosion in Southern Italy. The University of Texas at Austin., n.d. https://www.jstor.org/stable/24103320

Anon: In Toward an improved understanding of uplift mechanisms and the elevation history of the Tibetan Plateau (Vol. 507, pp. 23-58). Geological Society of America Special Papers., n.d.

Anon: Tectonics, Climate, and Landscape Evolution, Issue 398, n.d.

Anon: Wobus, C., Whipple, K. X., Kirby, E., Snyder, N., Johnson, J., Spyropolou, K., & Willett, S. D. (2006). Tectonics from topography: Procedures, promise, and pitfalls. Special papers-geological society of america, 398, 55., n.d.

Anon: Zeitler, P. K., Meltzer, A. S., Brown, L., Kidd, W. S., Lim, C., & Enkelmann, E. (2014). Tectonics and topographic evolution of Namche Barwa and the easternmost Lhasa block, Tibet., n.d.

Azor, A., Keller, E. A., and Yeats, R. S.: Geomorphic indicators of active fold growth: South Mountain–Oak Ridge anticline, Ventura basin, southern California, 114, 745–753, https://doi.org/10.1130/0016-7606(2002)114<0745: GIOAFG>2.0.CO;2, 2002.

Ballantyne, C. K.: Paraglacial geomorphology, Quaternary Science Reviews, 21, 1935–2017, https://doi.org/10.1016/S0277-3791(02)00005-7, 2002.

Benda, L. and Dunne, T.: Stochastic forcing of sediment supply to channel networks from landsliding and debris flow, Water Resour. Res., 33, 2849–2863, https://doi.org/10.1029/97WR02388, 1997.

https://doi.org/10.5194/egusphere-2022-533
Preprint. Discussion started: 12 July 2022

Bhatt, B. C. and Nakamura, K.: Characteristics of Monsoon Rainfall around the Himalayas Revealed by TRMM Precipitation Radar, 133, 149–165, https://doi.org/10.1175/MWR-2846.1, 2005.

Bilham, R., Gaur, V. K., and Molnar, P.: Himalayan Seismic Hazard, Science, 293, 1442–1444, https://doi.org/10.1126/science.1062584, 2001.

Bookhagen, B. and Burbank, D. W.: Topography, relief, and TRMM-derived rainfall variations along the Himalaya, Geophys. Res. Lett., 33, L08405, https://doi.org/10.1029/2006GL026037, 2006.

Bookhagen, B. and Burbank, D. W.: Toward a complete Himalayan hydrological budget: Spatiotemporal distribution of snowmelt and rainfall and their impact on river discharge, J. Geophys. Res., 115, F03019, https://doi.org/10.1029/2009JF001426, 2010.

Bookhagen, B., Thiede, R. C., and Strecker, M. R.: Abnormal monsoon years and their control on erosion and sediment flux in the high, arid northwest Himalaya, Earth and Planetary Science Letters, 231, 131–146, https://doi.org/10.1016/j.epsl.2004.11.014, 2005a.

Bookhagen, B., Thiede, R. C., and Strecker, M. R.: Late Quaternary intensified monsoon phases control landscape evolution in the northwest Himalaya, Geol, 33, 149, https://doi.org/10.1130/G20982.1, 2005b.

Borgatti, L. and Soldati, M.: Landslides as a geomorphological proxy for climate change: A record from the Dolomites (northern Italy), Geomorphology, 120, 56–64, https://doi.org/10.1016/j.geomorph.2009.09.015, 2010.

Brocklehurst, S. H. and Whipple, K. X.: Glacial erosion and relief production in the Eastern Sierra Nevada, California, Geomorphology, 42, 1–24, https://doi.org/10.1016/S0169-555X(01)00069-1, 2002.

Broeckx, J., Rossi, M., Lijnen, K., Campforts, B., Poesen, J., and Vanmaercke, M.: Landslide mobilization rates: A global analysis and model, Earth-Science Reviews, 201, 102972, https://doi.org/10.1016/j.earscirev.2019.102972, 2020.

Burbank, D. W., Blythe, A. E., Putkonen, J., Pratt-Sitaula, B., Gabet, E., Oskin, M., Barros, A., and Ojha, T. P.: Decoupling of erosion and precipitation in the Himalayas, Nature, 426, 652–

655, https://doi.org/10.1038/nature02187, 2003.

Burbank, D. W., Leland, J., Fielding, E., Anderson, R. S., Brozovic, N., Reid, M. R., and Duncan, C.: Bedrock incision, rock uplift and threshold hillslopes in the northwestern Himalayas, Nature, 379, 505–510, https://doi.org/10.1038/379505a0, 1996.

Burbank, D. W.: Rates of erosion and their implications for exhumation, Mineral. mag., 66, 25–52, https://doi.org/10.1180/0026461026610014, 2002.

Campforts, B., Shobe, C. M., Steer, P., Vanmaercke, M., Lague, D., and Braun, J.: HyLands 1.0: a hybrid landscape evolution model to simulate the impact of landslides and landslide-derived sediment on landscape evolution, Geosci. Model Dev., 13, 3863–3886, https://doi.org/10.5194/gmd-13-3863-2020, 2020.

Champagnac, J.-D., Molnar, P., Sue, C., and Herman, F.: Tectonics, climate, and mountain topography: TECTONICS CLIMATE MOUNTAIN TOPOGRAPHY, J. Geophys. Res., 117, n/a-n/a, https://doi.org/10.1029/2011JB008348, 2012.

Champel, B.: Growth and lateral propagation of fault-related folds in the Siwaliks of western Nepal: Rates, mechanisms, and geomorphic signature, J. Geophys. Res., 107, 2111, https://doi.org/10.1029/2001JB000578, 2002.

Croissant, T., Lague, D., Steer, P., and Davy, P.: Rapid post-seismic landslide evacuation boosted by dynamic river width, Nature Geosci, 10, 680–684, https://doi.org/10.1038/ngeo3005, 2017.

Croissant, T., Steer, P., Lague, D., Davy, P., Jeandet, L., and Hilton, R. G.: Seismic cycles, earthquakes, landslides and sediment fluxes: Linking tectonics to surface processes using a reduced-complexity model, Geomorphology, 339, 87–103, https://doi.org/10.1016/j.geomorph.2019.04.017, 2019a.

Croissant, T., Steer, P., Lague, D., Davy, P., Jeandet, L., and Hilton, R. G.: Seismic cycles, earthquakes, landslides and sediment fluxes: Linking tectonics to surface processes using a reduced-complexity model, Geomorphology, 339, 87–103, https://doi.org/10.1016/j.geomorph.2019.04.017, 2019b.

Crozier, M. J. and Glade, T.: Frequency and magnitude of landsliding: fundamental research issues, zfg_suppl0, 115, 141–155, https://doi.org/10.1127/zfgsuppl/115/1999/141, 1999.

Densmore, A. L. and Hovius, N.: Topographic fingerprints of bedrock landslides, Geol, 28, 371, https://doi.org/10.1130/0091-7613(2000)28<371: TFOBL>2.0.CO;2, 2000.

Dimri, A. P., Chevuturi, A., Niyogi, D., Thayyen, R. J., Ray, K., Tripathi, S. N., Pandey, A. K., and Mohanty, U. C.: Cloudbursts in Indian Himalayas: A review, Earth-Science Reviews, 168, 1–23, https://doi.org/10.1016/j.earscirev.2017.03.006, 2017.

Dimri, A. P., Niyogi, D., Barros, A. P., Ridley, J., Mohanty, U. C., Yasunari, T., and Sikka, D. R.: Western Disturbances: A review: WESTERN DISTURBANCE: A REVIEW, Rev. Geophys., 53, 225–246, https://doi.org/10.1002/2014RG000460, 2015.

Egholm, D. L., Knudsen, M. F., and Sandiford, M.: Lifespan of mountain ranges scaled by feedbacks between landsliding and erosion by rivers, Nature, 498, 475–478, https://doi.org/10.1038/nature12218, 2013.

Flint, J. J.: Stream gradient as a function of order, magnitude, and discharge, Water Resour. Res., 10, 969–973, https://doi.org/10.1029/WR010i005p00969, 1974.

Frank, W., Hoinkes, G., Miller, C., Purtscheller, F., Richter, W., and Th�ni, M.: Relations between metamorphism and orogeny in a typical section of the Indian Himalayas, TMPM Tschermaks Petr. Mitt., 20, 303–332, https://doi.org/10.1007/BF01081339, 1973.

Gadgil, S.: The Indian Monsoon and Its Variability, Annu. Rev. Earth Planet. Sci., 31, 429–467, https://doi.org/10.1146/annurev.earth.31.100901.141251, 2003.

Garzanti, E., Vezzoli, G., Andò, S., Paparella, P., and Clift, P. D.: Petrology of Indus River sands: a key to interpret erosion history of the Western Himalayan Syntaxis, Earth and Planetary Science Letters, 229, 287–302, https://doi.org/10.1016/j.epsl.2004.11.008, 2005.

Ghimire, S., Choudhary, A., and Dimri, A. P.: Assessment of the performance of CORDEX-South Asia experiments for monsoonal precipitation over the Himalayan region during present climate: part I, Clim Dyn, 50, 2311–2334, https://doi.org/10.1007/s00382-015-2747-2, 2018.

Glade, R. C., Shobe, C. M., Anderson, R. S., and Tucker, G. E.: Canyon shape and erosion dynamics governed by channel-hillslope feedbacks, 47, 650–654, https://doi.org/10.1130/G46219.1, 2019.

Godard, V., Bourles, D. L., Spinabella, F., Burbank, D. W., Bookhagen, B., Fisher, G. B., Moulin, A., and Leanni, L.: Dominance of tectonics over climate in Himalayan denudation, Geology, 42, 243–246, https://doi.org/10.1130/G35342.1, 2014.

Godard, V., Cattin, R., and Lavé, J.: Numerical modeling of mountain building: Interplay between erosion law and crustal rheology: INTERPLAY BETWEEN EROSION AND RHEOLOGY, Geophys. Res. Lett., 31, https://doi.org/10.1029/2004GL021006, 2004.

Gupta, V. and Sah, M. P.: Impact of the Trans-Himalayan Landslide Lake Outburst Flood (LLOF) in the Satluj catchment, Himachal Pradesh, India, Nat Hazards, 45, 379–390, https://doi.org/10.1007/s11069-007-9174-6, 2008a.

Gupta, V. and Sah, M. P.: Impact of the Trans-Himalayan Landslide Lake Outburst Flood (LLOF) in the Satluj catchment, Himachal Pradesh, India, Nat Hazards, 45, 379–390, https://doi.org/10.1007/s11069-007-9174-6, 2008b.

Guzzetti, F., Reichenbach, P., Ardizzone, F., Cardinali, M., and Galli, M.: Estimating the quality of landslide susceptibility models, Geomorphology, 81, 166–184, https://doi.org/10.1016/j.geomorph.2006.04.007, 2006.

Hancock, G. S. and Anderson, R. S.: Numerical modeling of fluvial strath-terrace formation in response to oscillating climate, 114, 1131–1142, https://doi.org/10.1130/0016-7606(2002)114<1131: NMOFST>2.0.CO;2, 2002.

Harvey, A. M.: Effective timescales of coupling within fluvial systems, Geomorphology, 44, 175–201, https://doi.org/10.1016/S0169-555X(01)00174-X, 2002.

Hodges, K. V., Hurtado, J. M., and Whipple, K. X.: Southward extrusion of Tibetan crust and its effect on Himalayan tectonics, Tectonics, 20, 799–809, https://doi.org/10.1029/2001TC001281, 2001.

Hodges, K. V., Wobus, C., Ruhl, K., Schildgen, T., and Whipple, K.: Quaternary deformation, river steepening, and heavy precipitation at the front of the Higher Himalayan ranges, Earth and Planetary Science Letters, 220, 379–389, https://doi.org/10.1016/S0012-821X(04)00063-9, 2004.

Hovius, N., Meunier, P., Lin, C.-W., Chen, H., Chen, Y.-G., Dadson, S., Horng, M.-J., and

https://doi.org/10.5194/egusphere-2022-533
Preprint. Discussion started: 12 July 2022

Lines, M.: Prolonged seismically induced erosion and the mass balance of a large earthquake, Earth and Planetary Science Letters, 304, 347–355, https://doi.org/10.1016/j.epsl.2011.02.005, 2011.

Hovius, N., Stark, C. P., and Allen, P. A.: Sediment flux from a mountain belt derived by landslide mapping, Geol, 25, 231, https://doi.org/10.1130/0091-7613(1997)025<0231:SFFAMB>2.3.CO;2, 1997.

Howard, A. D. and Kerby, G.: Channel changes in badlands, Geol Soc America Bull, 94, 739, https://doi.org/10.1130/0016-7606(1983)94<739: CCIB>2.0.CO;2, 1983.

Iwahashi, J., Watanabe, S., and Furuya, T.: Mean slope-angle frequency distribution and size frequency distribution of landslide masses in Higashikubiki area, Japan, Geomorphology, 50, 349–364, https://doi.org/10.1016/S0169-555X(02)00222-2, 2003.

Jaiswara, N. K., Kotluri, S. K., Pandey, A. K., and Pandey, P.: Transient basin as indicator of tectonic expressions in bedrock landscape: Approach based on MATLAB geomorphic tool (Transient-profiler), Geomorphology, 346, 106853, https://doi.org/10.1016/j.geomorph.2019.106853, 2019b.

Jaiswara, N. K., Kotluri, S. K., Pandey, P., and Pandey, A. K.: MATLAB functions for extracting hypsometry, stream-length gradient index, steepness index, chi gradient of channel and swath profiles from digital elevation model (DEM) and other spatial data for landscape characterisation, Applied Computing and Geosciences, 7, 100033, https://doi.org/10.1016/j.acags.2020.100033, 2020.

Jaiswara, N. K., Pandey, P., and Pandey, A. K.: Mio-Pliocene piracy, relict landscape and drainage reorganization in the Namcha Barwa syntaxis zone of eastern Himalaya, Sci Rep, 9, 17585, https://doi.org/10.1038/s41598-019-54052-x, 2019a.

Jamir, I., Gupta, V., Kumar, V., and Thong, G. T.: Evaluation of potential surface instability using finite element method in Kharsali Village, Yamuna Valley, Northwest Himalaya, J. Mt. Sci., 14, 1666–1676, https://doi.org/10.1007/s11629-017-4410-3, 2017.

Kirby, E. and Whipple, K. X.: Expression of active tectonics in erosional landscapes, Journal of Structural Geology, 44, 54–75, https://doi.org/10.1016/j.jsg.2012.07.009, 2012.

https://doi.org/10.5194/egusphere-2022-533
Preprint. Discussion started: 12 July 2022

Korup, O., Densmore, A. L., and Schlunegger, F.: The role of landslides in mountain range evolution, Geomorphology, 120, 77–90, https://doi.org/10.1016/j.geomorph.2009.09.017, 2010b.

Korup, O., Montgomery, D. R., and Hewitt, K.: Glacier and landslide feedbacks to topographic relief in the Himalayan syntaxes, Proc. Natl. Acad. Sci. U.S.A., 107, 5317–5322, https://doi.org/10.1073/pnas.0907531107, 2010a.

Kumar, V., Gupta, V., and Jamir, I.: Hazard evaluation of progressive Pawari landslide zone, Satluj valley, Himachal Pradesh, India, Nat Hazards, 93, 1029–1047, https://doi.org/10.1007/s11069-018-3339-3, 2018.

Kumar, V., Gupta, V., and Sundriyal, Y. P.: Spatial interrelationship of landslides, litho-tectonics, and climate regime, Satluj valley, Northwest Himalaya, Geological Journal, 54, 537–551, https://doi.org/10.1002/gj.3204, 2019.

Lague, D., Hovius, N., and Davy, P.: Discharge, discharge variability, and the bedrock channel profile: DISCHARGE VARIABILITY AND CHANNEL PROFILE, J. Geophys. Res., 110, n/a-n/a, https://doi.org/10.1029/2004JF000259, 2005.

Larsen, I. J. and Montgomery, D. R.: Landslide erosion coupled to tectonics and river incision, Nature Geosci, 5, 468–473, https://doi.org/10.1038/ngeo1479, 2012.

Lehner, B., Verdin, K., and Jarvis, A.: New Global Hydrography Derived From Spaceborne Elevation Data, Eos Trans. AGU, 89, 93, https://doi.org/10.1029/2008EO100001, 2008.

Malik, Javed N., and Takashi Nakata. "Active faults and related Late Quaternary deformation along the northwestern Himalayan Frontal Zone, India." Annals of Geophysics (2003). http://hdl.handle.net/2122/996

Miller, C., Klötzli, U., Frank, W., Thöni, M., and Grasemann, B.: Proterozoic crustal evolution in the NW Himalaya (India) as recorded by circa 1.80 Ga mafic and 1.84 Ga granitic magmatism, Precambrian Research, 103, 191–206, https://doi.org/10.1016/S0301-9268(00)00091-7, 2000.

Miller, C., Thöni, M., Frank, W., Grasemann, B., Klötzli, U., Guntli, P., and Draganits, E.: The early Palaeozoic magmatic event in the Northwest Himalaya, India: source, tectonic setting

https://doi.org/10.5194/egusphere-2022-533
Preprint. Discussion started: 12 July 2022

and age of emplacement, Geol. Mag., 138, 237–251, https://doi.org/10.1017/S0016756801005283, 2001.

Milliman, J. D. and Meade, R. H.: World-Wide Delivery of River Sediment to the Oceans, The Journal of Geology, 91, 1–21, https://doi.org/10.1086/628741, 1983.

Montgomery, D. R.: Slope Distributions, Threshold Hillslopes, and Steady-state Topography, Am J Sci, 301, 432–454, https://doi.org/10.2475/ajs.301.4-5.432, 2001.

Morell, K. D., Sandiford, M., Rajendran, C. P., Rajendran, K., Alimanovic, A., Fink, D., and Sanwal, J.: Geomorphology reveals active décollement geometry in the central Himalayan seismic gap, Lithosphere, 7, 247–256, https://doi.org/10.1130/L407.1, 2015.

Nakata, T. (1972). Geomorphic history and crustal movement of the foot-hills of the Himalayas. Science Report Tohoku Univ. 7th series (Geography), 22, 39-177.

O'Callaghan, J. F., & Mark, D. M. (1984). The extraction of drainage networks from digital elevation data. Computer vision, graphics, and image processing, 28(3), 323-344.

Olen, S. M., Bookhagen, B., and Strecker, M. R.: Role of climate and vegetation density in modulating denudation rates in the Himalaya, Earth and Planetary Science Letters, 445, 57–67, https://doi.org/10.1016/j.epsl.2016.03.047, 2016.

Orr, E. N., Owen, L. A., Saha, S., and Caffee, M. W.: Rates of rockwall slope erosion in the upper Bhagirathi catchment, Garhwal Himalaya, Earth Surf. Process. Landforms, 44, 3108–3127, https://doi.org/10.1002/esp.4720, 2019.

Orr, E. N., Owen, L. A., Saha, S., Hammer, S. J., and Caffee, M. W.: Rockwall Slope Erosion in the Northwestern Himalaya, J. Geophys. Res. Earth Surf., 126, https://doi.org/10.1029/2020JF005619, 2021.

Ouimet, W. B., Whipple, K. X., Royden, L. H., Sun, Z., and Chen, Z.: The influence of large landslides on river incision in a transient landscape: Eastern margin of the Tibetan Plateau (Sichuan, China), Geological Society of America Bulletin, 119, 1462–1476, https://doi.org/10.1130/B26136.1, 2007.

Parkash, S.: Education, Training and Capacity Development for Mainstreaming Landslides Risk Management, in: Landslide Science and Practice, edited by: Margottini, C., Canuti, P., and Sassa, K., Springer Berlin Heidelberg, Berlin, Heidelberg, 257–264, https://doi.org/10.1007/978-3-642-31313-4_33, 2013.

Pedersen, V. K. and Egholm, D. L.: Glaciations in response to climate variations preconditioned by evolving topography, Nature, 493, 206–210, https://doi.org/10.1038/nature11786, 2013.

Rao, S. V. N., Rao, M. V., Ramasastri, K. S., and Singh, R. N. P.: A Study of Sedimentation in Chenab Basin in Western Himalayas, 28, 201–216, https://doi.org/10.2166/nh.1997.0012, 1997.

Reid, L. M. and Page, M. J.: Magnitude and frequency of landsliding in a large New Zealand catchment, Geomorphology, 49, 71–88, https://doi.org/10.1016/S0169-555X(02)00164-2, 2003.

Roback, K., Clark, M. K., West, A. J., Zekkos, D., Li, G., Gallen, S. F., Chamlagain, D., and Godt, J. W.: The size, distribution, and mobility of landslides caused by the 2015 Mw7.8 Gorkha earthquake, Nepal, Geomorphology, 301, 121–138, https://doi.org/10.1016/j.geomorph.2017.01.030, 2018.

Safran, E. B., Bierman, P. R., Aalto, R., Dunne, T., Whipple, K. X., and Caffee, M.: Erosion rates driven by channel network incision in the Bolivian Andes, Earth Surf. Process. Landforms, 30, 1007–1024, https://doi.org/10.1002/esp.1259, 2005.

Sanchez, G., Rolland, Y., Corsini, M., Braucher, R., Bourlès, D., Arnold, M., and Aumaître, G.: Relationships between tectonics, slope instability and climate change: Cosmic ray exposure dating of active faults, landslides and glacial surfaces in the SW Alps, Geomorphology, 117, 1–13, https://doi.org/10.1016/j.geomorph.2009.10.019, 2010.

Saylor, J., DeCelles, P., Gehrels, G., Murphy, M., Zhang, R., and Kapp, P.: Basin formation in the High Himalaya by arc-parallel extension and tectonic damming: Zhada basin, southwestern Tibet: ZHADA EVOLUTION ARC-PARALLEL EXTENSION, Tectonics, 29, n/a-n/a, https://doi.org/10.1029/2008TC002390, 2010.

Scherler, D., Bookhagen, B., and Strecker, M. R.: Spatially variable response of Himalayan glaciers to climate change affected by debris cover, Nature Geosci, 4, 156–159, https://doi.org/10.1038/ngeo1068, 2011.

https://doi.org/10.5194/egusphere-2022-533
Preprint. Discussion started: 12 July 2022

Scherler, D., Bookhagen, B., and Strecker, M. R.: Tectonic control on ^{10}Be-derived erosion rates in the Garhwal Himalaya, India: GARHWAL HIMALAYA EROSION RATES, J. Geophys. Res. Earth Surf., 119, 83–105, https://doi.org/10.1002/2013JF002955, 2014.

Scherler, D., Bookhagen, B., Strecker, M. R., von Blanckenburg, F., and Rood, D.: Timing and extent of late Quaternary glaciation in the western Himalaya constrained by 10Be moraine dating in Garhwal, India, Quaternary Science Reviews, 29, 815–831, https://doi.org/10.1016/j.quascirev.2009.11.031, 2010.

Schlup, M., Carter, A., Cosca, M., and Steck, A.: Exhumation history of eastern Ladakh revealed by ^{40}Ar/^{39}Ar and fission-track ages: the Indus River–Tso Morari transect, NW Himalaya, Journal of the Geological Society, 160, 385–399, https://doi.org/10.1144/0016-764902-084, 2003.

Schumm, S. A.: Geomorphic Thresholds: The Concept and Its Applications, Transactions of the Institute of British Geographers, 4, 485, https://doi.org/10.2307/622211, 1979.

Schwanghart, W. and Scherler, D.: Short Communication: TopoToolbox 2 – MATLAB-based software for topographic analysis and modeling in Earth surface sciences, Earth Surf. Dynam., 2, 1–7, https://doi.org/10.5194/esurf-2-1-2014, 2014.

Searle, M. P. and Fryer, B. J.: Garnet, tourmaline and muscovite-bearing leucogranites, gneisses and migmatites of the Higher Himalayas from Zanskar, Kulu, Lahoul and Kashmir, Geological Society, London, Special Publications, 19, 185–201, https://doi.org/10.1144/GSL.SP.1986.019.01.10, 1986.

Searle, M. P.: Structural evolution and sequence of thrusting in the High Himalayan, Tibetan—Tethys and Indus suture zones of Zanskar and Ladakh, Western Himalaya, Journal of Structural Geology, 8, 923–936, https://doi.org/10.1016/0191-8141(86)90037-4, 1986.

Searle, M., Corfield, R. I., Stephenson, B. E. N., & McCarron, J. O. E. (1997). Structure of the North Indian continental margin in the Ladakh–Zanskar Himalayas: implications for the timing of obduction of the Spontang ophiolite, India–Asia collision and deformation events in the Himalaya. Geological Magazine, 134(3), 297-316.

Seeber, L. and Armbruster, J. G.: Great Detachment Earthquakes Along the Himalayan Arc and Long-Term Forecasting, in: Maurice Ewing Series, edited by: Simpson, D. W. and

https://doi.org/10.5194/egusphere-2022-533
Preprint. Discussion started: 12 July 2022

Richards, P. G., American Geophysical Union, Washington, D. C., 259–277, https://doi.org/10.1029/ME004p0259, 2013.

Seeber, L. and Gornitz, V.: River profiles along the Himalayan arc as indicators of active tectonics, Tectonophysics, 92, 335–367, https://doi.org/10.1016/0040-1951(83)90201-9, 1983.

Shobe, C. M., Tucker, G. E., and Anderson, R. S.: Hillslope-derived blocks retard river incision, Geophys. Res. Lett., 43, 5070–5078, https://doi.org/10.1002/2016GL069262, 2016.

Shroder, J. F. and Bishop, M. P.: Mass movement in the Himalaya: new insights and research directions, Geomorphology, 26, 13–35, https://doi.org/10.1016/S0169-555X(98)00049-X, 1998.

Singh, P. and Kumar, N.: Effect of orography on precipitation in the western Himalayan region, Journal of Hydrology, 199, 183–206, https://doi.org/10.1016/S0022-1694(96)03222-2, 1997.

Small, E. E. and Anderson, R. S.: Pleistocene relief production in Laramide mountain ranges, western United States, Geol, 26, 123, https://doi.org/10.1130/0091-7613(1998)026<0123: PRPILM>2.3.CO;2, 1998.

Snyder, N. P., Whipple, K. X., Tucker, G. E., and Merritts, D. J.: Landscape response to tectonic forcing: Digital elevation model analysis of stream profiles in the Mendocino triple junction region, northern California, Geological Society of America Bulletin, 112, 1250–1263, https://doi.org/10.1130/0016-7606(2000)112<1250: LRTTFD>2.0.CO;2, 2000.

Snyder, N. P., Whipple, K. X., Tucker, G. E., and Merritts, D. J.: Channel response to tectonic forcing: field analysis of stream morphology and hydrology in the Mendocino triple junction region, northern California, Geomorphology, 53, 97–127, https://doi.org/10.1016/S0169-555X(02)00349-5, 2003.

Stark, C. P. and Hovius, N.: The characterization of landslide size distributions, Geophys. Res. Lett., 28, 1091–1094, https://doi.org/10.1029/2000GL008527, 2001.

Steck, A., MatthieuGirard, A. M., & Robyr, M. (1998). Geological transect across the Tso Morari and Spiti areas: Thenappe structures of the Tethys Himalaya. Eclogae Geol. Helv., 91, 103-121.

Strahler, A. N.: HYPSOMETRIC (AREA-ALTITUDE) ANALYSIS OF EROSIONAL

https://doi.org/10.5194/egusphere-2022-533
Preprint. Discussion started: 12 July 2022

TOPOGRAPHY, Geol Soc America Bull, 63, 1117, https://doi.org/10.1130/0016-7606(1952)63 [1117: HAAOET]2.0.CO;2, 1952.

Thiede, R. C., Bookhagen, B., Arrowsmith, J. R., Sobel, E. R., and Strecker, M. R.: Climatic control on rapid exhumation along the Southern Himalayan Front, Earth and Planetary Science Letters, 222, 791–806, https://doi.org/10.1016/j.epsl.2004.03.015, 2004.

Tucker, G. E. and Hancock, G. R.: Modelling landscape evolution, Earth Surf. Process. Landforms, 35, 28–50, https://doi.org/10.1002/esp.1952, 2010.

Tucker, G. E.: Drainage basin sensitivity to tectonic and climatic forcing: implications of a stochastic model for the role of entrainment and erosion thresholds, Earth Surf. Process. Landforms, 29, 185–205, https://doi.org/10.1002/esp.1020, 2004.

Turowski, J. M., Lague, D., and Hovius, N.: Cover effect in bedrock abrasion: A new derivation and its implications for the modeling of bedrock channel morphology, J. Geophys. Res., 112, F04006, https://doi.org/10.1029/2006JF000697, 2007.

Valdiya, K. S. (1999). Rising Himalaya: advent and intensification. Curr. Sci, 76(4).

Valdiya, K. S.: River piracy: Saraswati that disappeared, Reson, 1, 19–28, https://doi.org/10.1007/BF02835165, 1996.

Vannay, J.-C., Grasemann, B., Rahn, M., Frank, W., Carter, A., Baudraz, V., and Cosca, M.: Miocene to Holocene exhumation of metamorphic crustal wedges in the NW Himalaya: Evidence for tectonic extrusion coupled to fluvial erosion: TECTONICS AND EROSION IN THE NW HIMALAYA, Tectonics, 23, n/a-n/a, https://doi.org/10.1029/2002TC001429, 2004.

Walker, J. D., Martin, M. W., Bowring, S. A., Searle, M. P., Waters, D. J., and Hodges, K. V.: Metamorphism, Melting, and Extension: Age Constraints from the High Himalayan Slab of Southeast Zanskar and Northwest Lahaul, The Journal of Geology, 107, 473–495, https://doi.org/10.1086/314360, 1999.

Webster, P. J., Magaña, V. O., Palmer, T. N., Shukla, J., Tomas, R. A., Yanai, M., and Yasunari, T.: Monsoons: Processes, predictability, and the prospects for prediction, J. Geophys. Res., 103, 14451–14510, https://doi.org/10.1029/97JC02719, 1998.

Weidinger, J. T., Korup, O., Munack, H., Altenberger, U., Dunning, S. A., Tippelt, G., and

Lottermoser, W.: Giant rockslides from the inside, Earth and Planetary Science Letters, 389, 62–73, https://doi.org/10.1016/j.epsl.2013.12.017, 2014.

Whipple, K. X. and Tucker, G. E.: Dynamics of the stream-power river incision model: Implications for height limits of mountain ranges, landscape response timescales, and research needs, J. Geophys. Res., 104, 17661–17674, https://doi.org/10.1029/1999JB900120, 1999.

Wulf, H., Bookhagen, B., and Scherler, D.: Seasonal precipitation gradients and their impact on fluvial sediment flux in the Northwest Himalaya, Geomorphology, 118, 13–21, https://doi.org/10.1016/j.geomorph.2009.12.003, 2010.

Yin, A. and Harrison, T. M.: Geologic Evolution of the Himalayan-Tibetan Orogen, Annu. Rev. Earth Planet. Sci., 28, 211–280, https://doi.org/10.1146/annurev.earth.28.1.211, 2000.

Zhang, L., Xiao, T., He, J., and Chen, C.: Erosion-based analysis of breaching of Baige landslide dams on the Jinsha River, China, in 2018, Landslides, 16, 1965–1979, https://doi.org/10.1007/s10346-019-01247-y, 2019a.

Zhang, L., Xiao, T., He, J., and Chen, C.: Erosion-based analysis of breaching of Baige landslide dams on the Jinsha River, China, in 2018, Landslides, 16, 1965–1979, https://doi.org/10.1007/s10346-019-01247-y, 2019b.

https://doi.org/10.5194/egusphere-2022-533
Preprint. Discussion started: 12 July 2022

Figures:

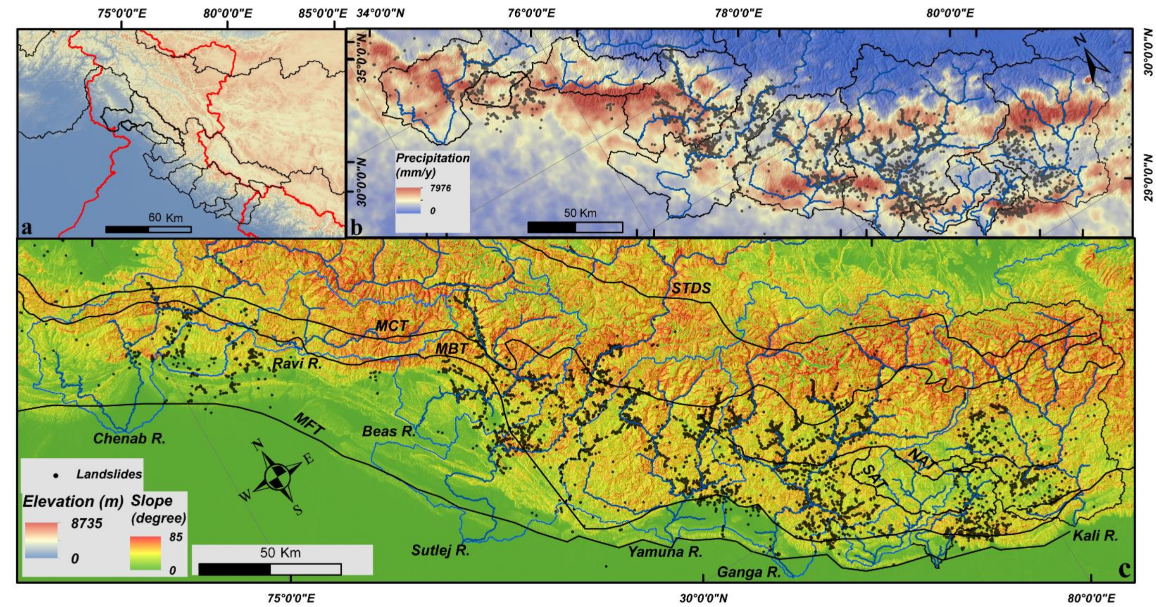

Fig.1: (a) The topography of the NW Himalaya-Tibet system overlaid with the studied river catchments such as Chenab, Beas, Sutlej, Yamuna, Ganga, and Kali (b) Spatial distribution of bedrock landslides (taken from bhukosh portal of GSI http://bhukosh.gsi.gov.in/) across annual mean precipitation overlaid with the studied river catchments (c) Spatial distribution of bedrock landslides across the slope gradient overlaid with the studied river catchments and tectonic boundary. Please note. (MFT= Main frontal thrust, MBT= Main boundary Thrust, MCT= Main Central Thrust, STDS= Southern Tibet Detachment system, NAT= North Almora Thrust, SAT= South Almora Thrust).

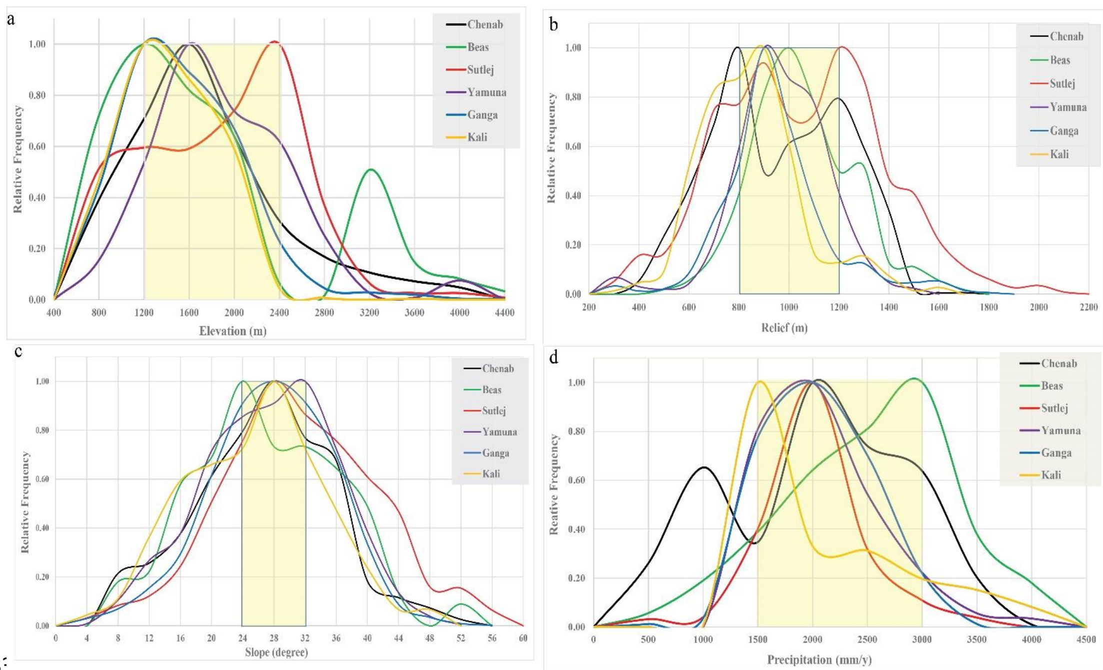

Fig.2. The relative distribution of bedrock landslides occurrences across (a) elevation (b) relief (c) slope (d) annual mean precipitation; in the studied river catchments

https://doi.org/10.5194/egusphere-2022-533
Preprint. Discussion started: 12 July 2022

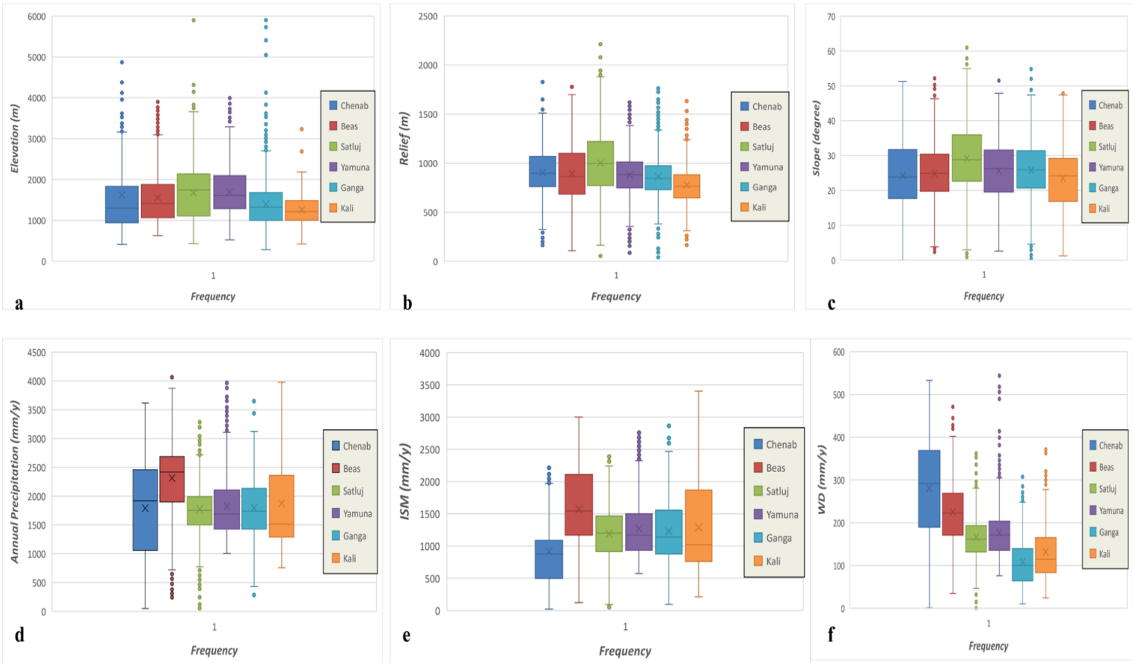

Fig.3. Statistical trend analysis of landslides occurrence points (from west to east) over (a) elevation (m) (b) relief (m) (c) slope (degree) (d) annual mean precipitation (e) Indian summer monsoon (f) Western disturbances; grids along studied river catchments, in NW Himalayas:

https://doi.org/10.5194/egusphere-2022-533
Preprint. Discussion started: 12 July 2022

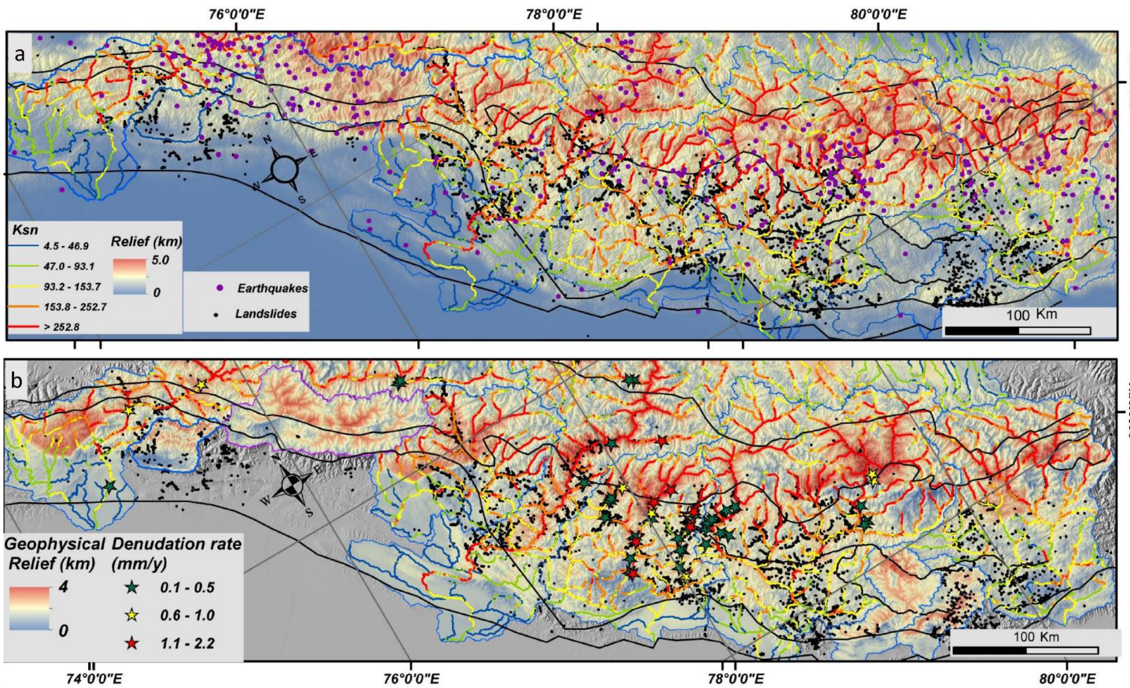

Fig.4. Spatial distribution of bedrock landslides across (a) topographic relief overlaid with Normalized steepness index (Ksn), earthquake distribution (taken from NASA-USGS open source platform) and tectonic boundary (b) geophysical relief overlaid with Normalized steepness index (Ksn), tectonic boundary and denudation rates (taken from previously published literatures referred: SM1) of the studied river catchments:

https://doi.org/10.5194/egusphere-2022-533
Preprint. Discussion started: 12 July 2022

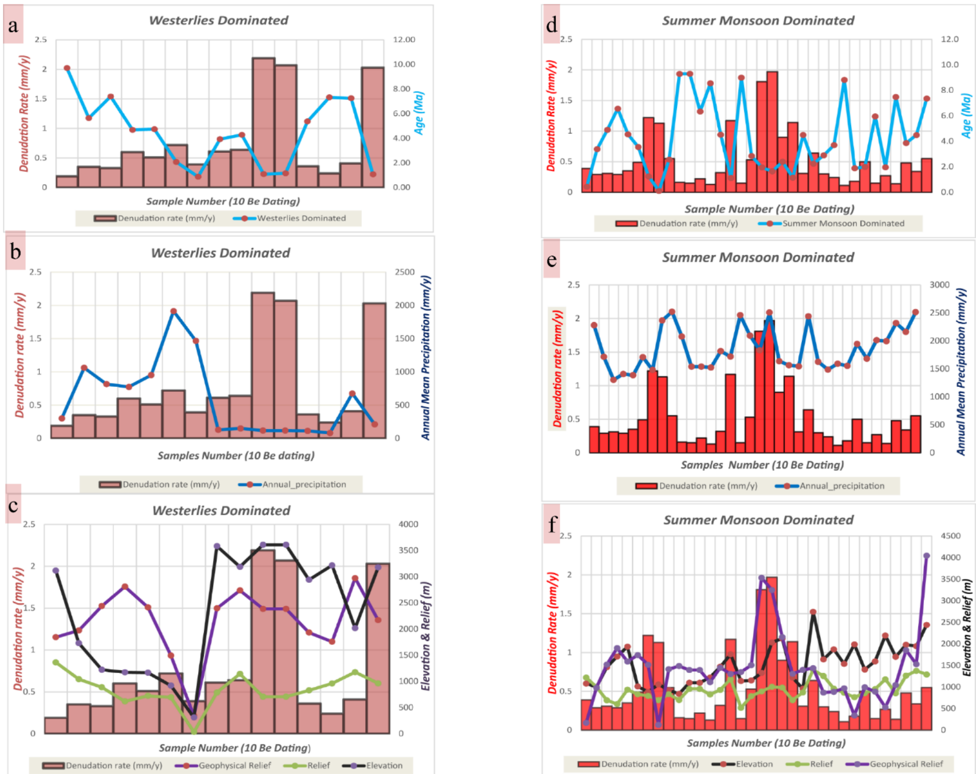

Fig.5. Spatial interrelationship of denudation rates across; westerlies dominated catchments with (a) exhumation age (b) annual mean precipitation (c) elevation & relief; Indian summer monsoon dominated catchments with (d) exhumation age (e) annual mean precipitation (f) elevation & relief:

https://doi.org/10.5194/egusphere-2022-533
Preprint. Discussion started: 12 July 2022

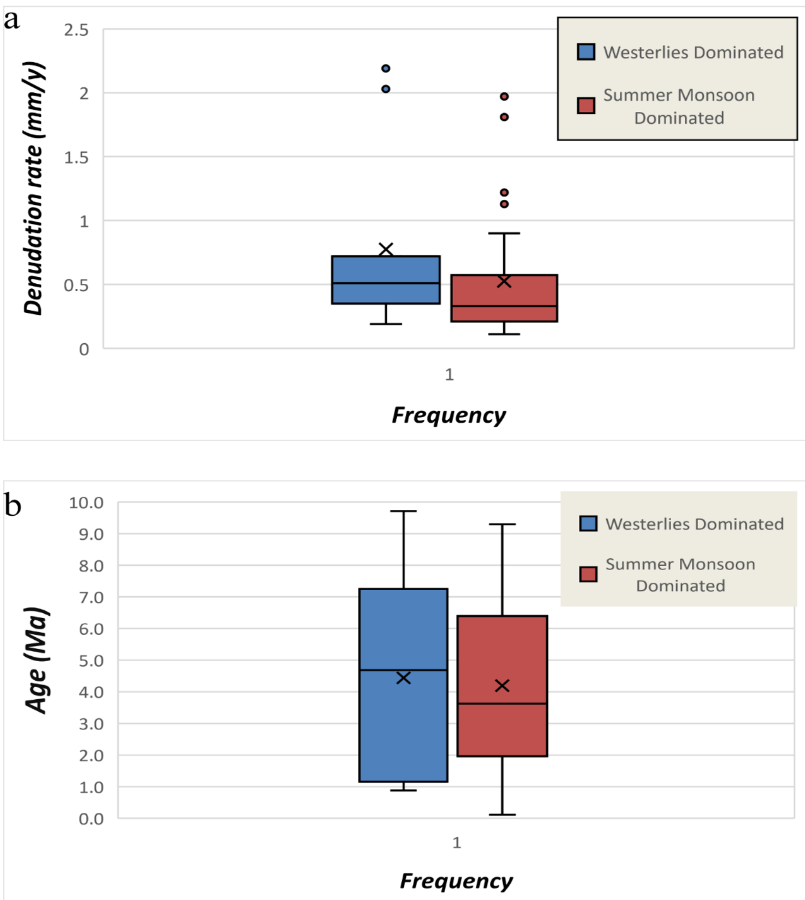

Fig. 6. Trend analysis of (a) Denudation rates across westerlies dominated catchments and Indian summer monsoon dominated catchments (b) Exhumation age across westerlies dominated catchments and Indian summer monsoon dominated catchments:

https://doi.org/10.5194/egusphere-2022-533
Preprint. Discussion started: 12 July 2022

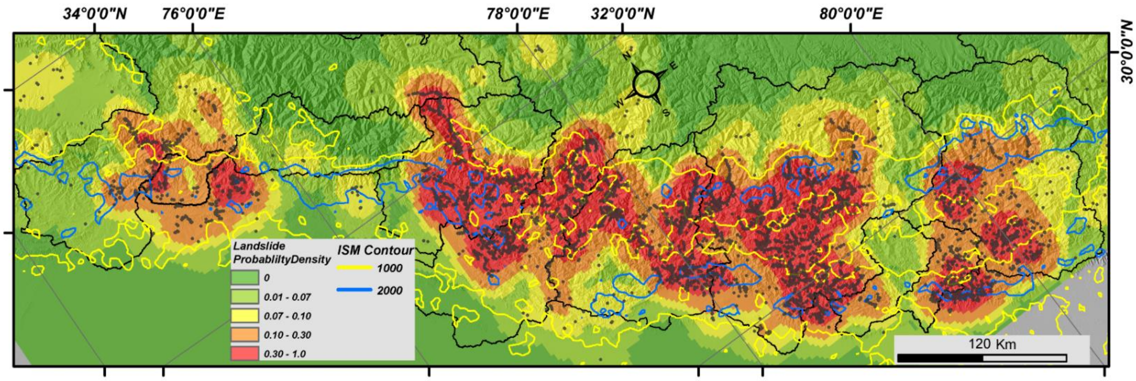

Fig. 7. Spatial distribution landslides probability density overlaid with Indian summer monsoon (ISM) contour intervals along with landslides points:

https://doi.org/10.5194/egusphere-2022-533
Preprint. Discussion started: 12 July 2022

Appendix:

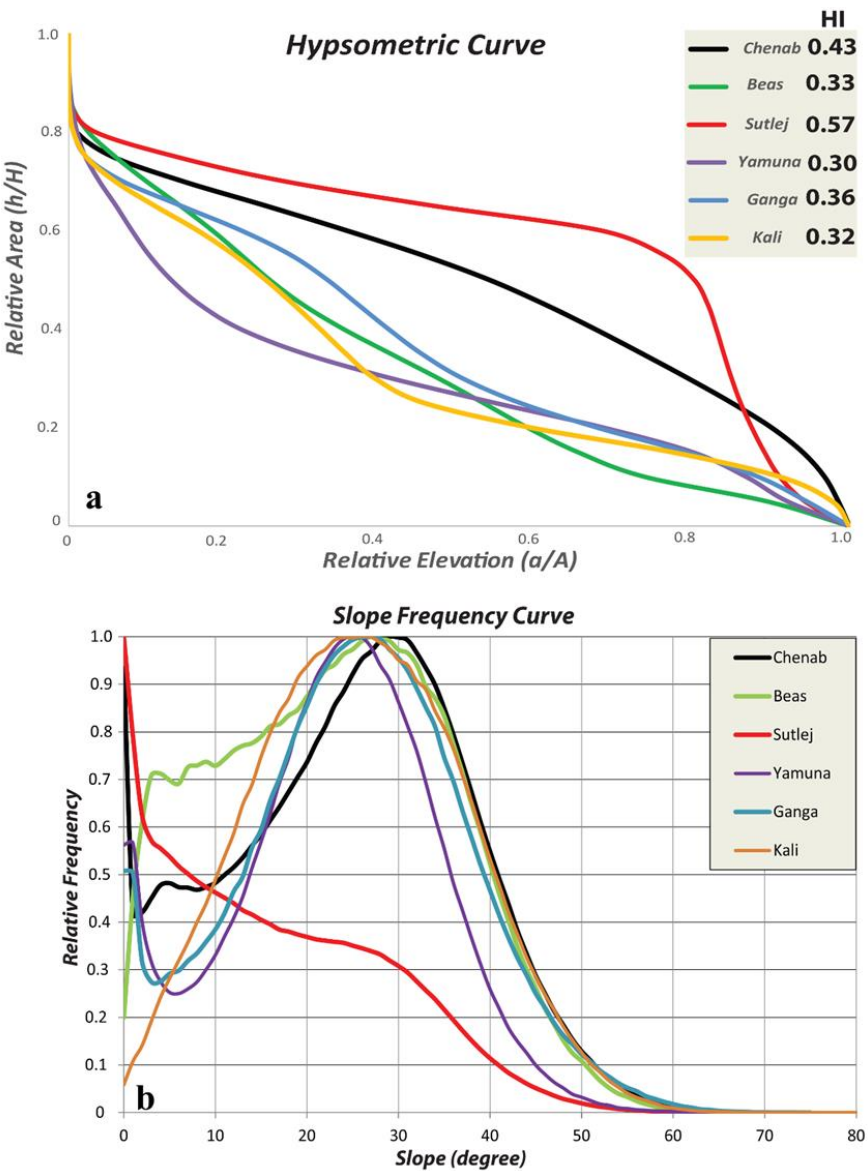

A1. (a) Hypsometric Curve and Hypsometric Integral of the studied river catchments: (b) Mean slope frequency curve of the studied river catchments:

https://doi.org/10.5194/egusphere-2022-533
Preprint. Discussion started: 12 July 2022

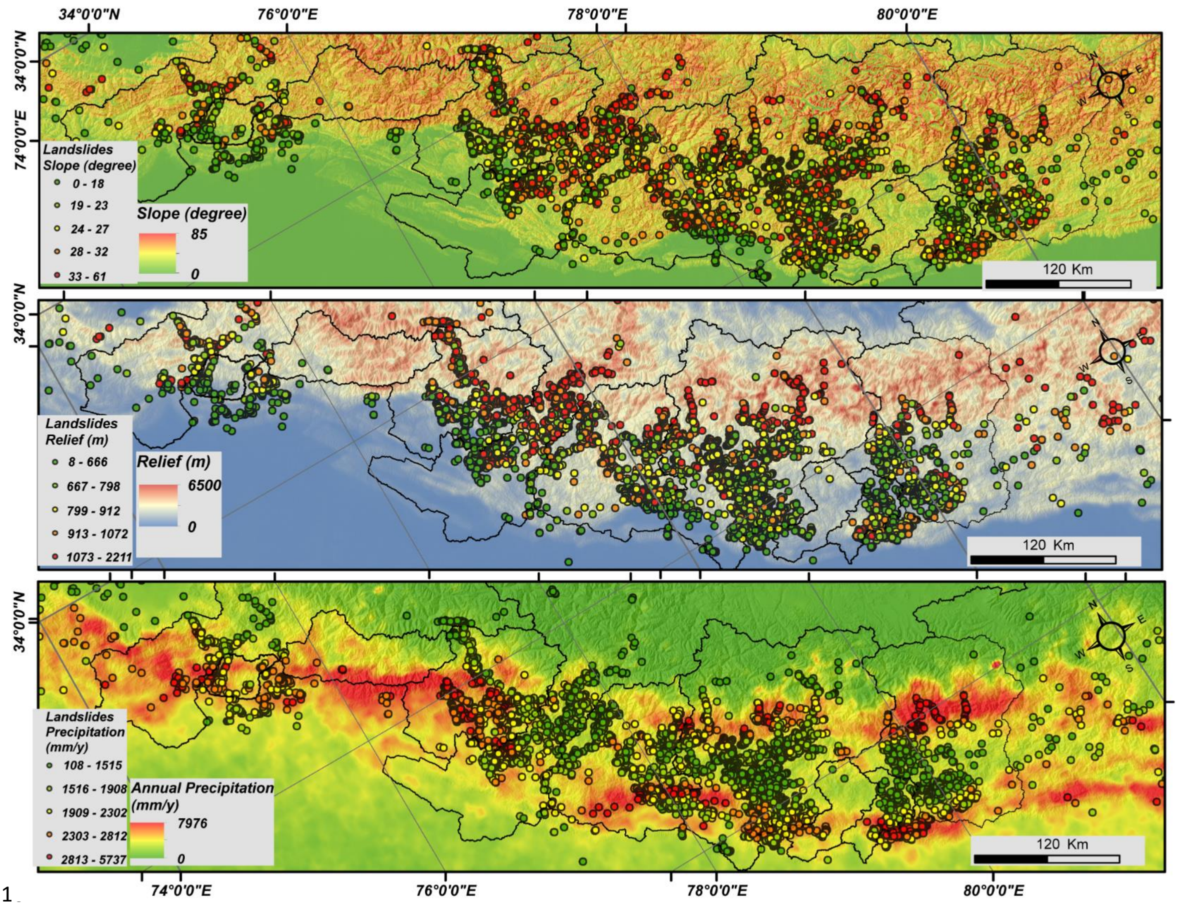

A2: Spatial classification of landslides occurrence points across (a) slope (b) relief (c) annual mean precipitation